Theoretical Studies on Structural, Magnetic, and Spintronic Characteristics of Sandwiched Eu_nCOT_{n+1} ($n = 1-4$) Clusters

Xiuyun Zhang,[†] Man-Fai Ng,[‡] Yanbiao Wang,[†] Jinlan Wang,[†,§,*] and Shuo-Wang Yang[‡,*]

[†]Department of Physics, Southeast University, Nanjing 211189, P. R. China, [‡]Institute of High Performance Computing, 1 Fusionopolis Way, No. 16-16 Connexis, Singapore 138632, Singapore, and [§]Shanghai Institute of Technical Physics, Chinese Academy of Sciences, Shanghai 200083, P.R. China

ABSTRACT Europium (Eu)-cyclootetatrene (COT = C_8H_8) multidecker clusters (Eu_nCOT_{n+1}, $n = 1-4$) are studied by relativistic density functional theory calculations. These clusters are found to be thermodynamically stable with freely rotatable COT rings, and their total magnetic moments (MMs) increase linearly along with the number of Eu atoms. Each Eu atom contributes about 7 μ_B to the cluster. Meanwhile, the internal COT rings have little MM contribution while the external COT rings have about 1 μ_B MM aligned in opposite direction to that of the Eu atoms. The total MM of the Eu_nCOT_{n+1} clusters can thus be generalized as $7n - 2$ μ_B where n is the number of Eu atoms. Besides, the ground states of these clusters are ferromagnetic and energetically competitive with the antiferromagnetic states, meaning that their spin states are very unstable, especially for larger clusters. More importantly, we uncover an interesting bonding characteristic of these clusters in which the interior ionic structure is capped by two hybrid covalent-ionic terminals. We suggest that such a characteristic makes the Eu_nCOT_{n+1} clusters extremely stable. Finally, we reveal that for the positively charged clusters, the hybrid covalent-ionic terminals will tip further toward the interior part of the clusters to form deeper covalent-ionic caps. In contrast, the negatively charged clusters turn to pure ionic structures.

KEYWORDS: sandwich clusters · magnetic moment · lanthanide compounds · density functional theory

Metal−organic ligand clusters are of ever-growing interest in recent years owing to their fundamental part in organometallic chemistry and potential or real applications in industry. Among them, multidecker organometallic sandwich clusters are intriguing species for their unique structural, electronic, magnetic, and optical properties.[1−27] For example, benzene−vanadium V_nBz_{n+1} cluster and its infinite $(VBz)_\infty$ one-dimensional (1D) wire have been the most well studied.[1−14] Recently, its ferrocene analogue $(FeCp)_\infty$ has been theoretically predicted to be the first sandwich molecular wire (SMW) with half-metallicity, high spin filter and negative differential resistance effects simultaneously.[15] At the same time, various multidecker sandwich molecular clusters and SMWs have been reported such as $V_{2n}Ant_{n+1}$ (Ant = anthracene), $TM_n(FeCp_2)_{n+1}$ (TM = transition metal; Cp = cyclopentadienyl), lanthanide (Ln)-COT (COT = cyclootetatrene or C_8H_8) clusters and hybrid SMW $(TMCpFeCp)_\infty$ where TM = Sc, Ti, V, and Mn.[16−24] Very recently, V-borazine SMW, which is actually an inorganic SMW, was reported to be half metallic and an almost perfect spin filter when graphene is used as the electrodes.[28,29] Obviously, 1D SMWs are promising candidates for next generation molecular electronics and spintronics because of the aforementioned unique properties.

Although sandwich molecular clusters composed of first row transition metals are of much interest currently, it is reported recently that 4f Ln-COT clusters have exhibited unusual properties, such as, large magnetic moment (MM) and extreme stability. For example, Stern−Gerlach magnetic deflection experiments[23,24] show that the Ln_nCOT_m clusters (Ln = Eu, Tb, Ho and Tm; $n = 1-7$) possess high MMs. In particular, the MM of the Eu_nCOT_{n+1} clusters increases linearly with its size. Besides, an 18-layer 1D Eu_nCOT_{n+1} wire was successfully synthesized by laser vaporization method.[22] In fact, recent mass spectra of Ln_nCOT_{n+1} (Ln = Ce, Nd, Eu, Ho, and Yb) clusters suggested that they are particularly stable and adopt 1D multidecker sandwich structures at a ratio of n:($n + 1$).[18] In addition, photoelectron spectra (PES) of $LnCOT_2^-$ clusters showed that the oxidation states of the Ln atoms are +2 for the Eu and Yb atoms while +3 for other Ln elements.[18] Chemical probe method on Na-adduct Ln_nCOT_{n+1} (Ln = Eu and Ho) clusters also confirmed that the Eu and Ho atoms exist as the Eu^{2+} and Ho^{3+}

*Address correspondence to jlwang@sec.edu.cn, yangsw@ihpc.a-star.edu.sg.

Received for review April 23, 2009 and accepted August 10, 2009.

Published online August 17, 2009.
10.1021/nn900401b CCC: $40.75

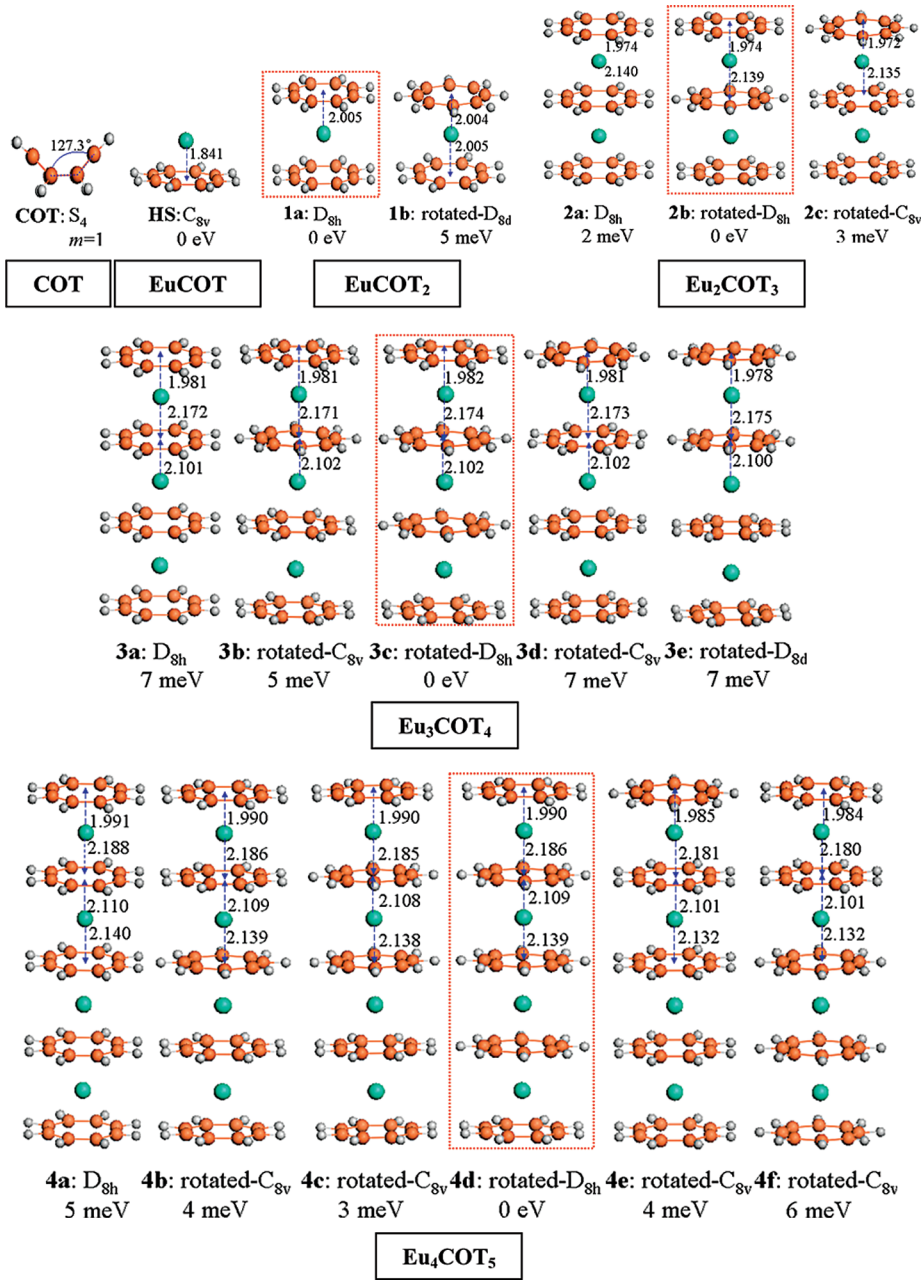

Figure 1. Optimized structures of COT and Eu_nCOT_{n+1} (n = 1−4). The labels show the symmetry and the relative energies of the clusters with respect to their ground state structures (embedded by dotted red boxes). Bond lengths are shown on the figures.

ions within the clusters, respectively.[19] Furthermore, the combined PES and DFT studies indicated the ionic bonding features in the open one-ended neutral and anionic Eu_nCOT_n (n = 1−4) sandwich clusters.[20,21]

Theoretical investigations on Ln-COT systems are relatively scarce and are mostly limited to small sizes.[25−27] Large-scale complete-active-space self-consistent field calculations on neutral and anionic Ln-COT_2 (Ln = Ce, Nd, Tb and Yb) clusters indicated that all the lanthanide atoms are trivalent (Ln^{3+}) rather than tetravalent as observed in actinide elements.[25] The ground electronic states of $LnCOT_2$ (Ln = Nd, Tb and Yb) are of $4f^n\pi^3$ configuration. It is different from that of the actinocene analogues, $UCOT_2$, which have the $5f^{n-1}\pi^4$ configuration.[26] More recently, DFT study showed that the direction of magnetization in Eu_2COT_3 clusters can be manipulated by changing their oxidation states.[27] However, many puzzles still remain for the Eu_nCOT_{n+1} clusters, such as (1) why do these clusters show huge MM and is there any obstacle for them in real applications, and (2) what are the bonding characteristics within the Eu_nCOT_{n+1} clusters?

In this work, we explore the structural, electronic, and magnetic properties of half-sandwich EuCOT and full-sandwich Eu_nCOT_{n+1} (n = 1−4) clusters by relativistic DFT calculations. Our results show that the total MM of these clusters increase linearly with the number of Eu atoms. Also, the ferromagnetic and antiferromagnetic states of these clusters are energetically competitive, indicating that their spin states are very unstable, especially for larger clusters. More importantly, we reveal an interesting bonding characteristic of these clusters: an ionic interior structure capped with two hybrid covalent-ionic terminals. Such unique structure in the Eu_nCOT_{n+1} clusters makes it extremely stable. Furthermore, our charge effect study shows that the hybrid covalent-ionic terminals will extend further toward the interior part of the cluster to form deeper covalent-ionic caps in the positively charged clusters. In contrast, the negatively charged clusters show pure ionic structure.

RESULTS AND DISCUSSION

Structure of Eu_nCOT_{n+1} Clusters. All the Eu_nCOT_{n+1} clusters considered in this work are shown in Figure 1. The ground-state structure of the COT ring is a boat configuration with S_4 symmetry (structure **COT**). Four carbon and four hydrogen atoms are drawn out of the molecular plane with an angle of 127.3° among the three adjacent carbon atoms. The alternating C−C bond lengths are 1.346 and 1.467 Å, which agrees with the results obtained by Pierrefixe *et al.*[30] Such nonplanar structure is

attributed to the antiaromaticity of the COT ring [8π ($4n$) electrons]. A stable aromatic ring should satisfy Hückel rule with $(4n + 2)\pi$ electrons in the system where n is integer. A planar structure of neutral COT ring is found to have a triplet spin state. However, this structure is 0.45 eV higher in energy than the boat-shaped ground state.

By adding a Eu atom above the COT ring, a stable half-sandwich EuCOT cluster is formed (structure **HS**). The cluster has an octet spin state with C_{8v} symmetry. The Eu atom is 1.841 Å above the mass center of the COT ring, where the C−C bond length in this structure is 1.406 Å and the C−H bond length is 1.075 Å.

For the $EuCOT_2$ cluster, there are two stable configurations: an eclipsed conformation (structure **1a**) with D_{8h} symmetry and a staggered conformation (structure **1b**) with D_{8d} symmetry where one COT ring is rotated by 22.5° along the 8-fold axis. Both **1a** and **1b** are found to be sextet spin states, and **1a** is the ground state but only exhibits 5.0 meV more favorable than **1b** in energy. Meanwhile, the distances between the Eu atom and mass center of the COT ring are almost the same (2.005 Å) in both **1a** and **1b**. Besides, we also consider the higher spin states by altering the spin state of **1a** to octet without changing the symmetry. The calculated result shows it is 0.28 eV higher than the sextet state in energy.

For the Eu_2COT_3, Eu_3COT_4, and Eu_4COT_5 clusters, we consider possible eclipsed and staggered conformations of the COT rings within the clusters (Figure 1). We find that the structure with the eclipsed internal COT rings, which are staggered to the two terminal COT rings (D_{8h} symmetry), is energetically most stable. They are structures **2b**, **3c**, and **4d** for the Eu_2COT_3, Eu_3COT_4, and Eu_4COT_5 clusters, respectively. However, the energy differences of the conformers among each cluster group are differed by at most 7 meV only. It implies that the COT rings can freely rotate at room temperature and it may be an advantage for practical applications since we do not need to consider the impact of COT rotations. In the following sections, we mainly consider the most stable conformer for each cluster group unless we indicate it specifically.

Stability of Eu_nCOT_{n+1} Clusters. The average binding energies (BE) for the Eu_nCOT_{n+1} clusters with respect to the individual Eu atom and COT ring are computed using the formula:

$$BE(n, n+1) = \{nE[Eu] + (n+1)E[COT] - E[Eu_nCOT_{n+1}]\}/n$$

where $E[Eu_nCOT_{n+1}]$, $E[COT]$, and $E[Eu]$ are the total energies of the optimized Eu_nCOT_{n+1} clusters, COT rings, and Eu atoms, respectively. The results are given in Table 1. The binding energy is 3.82 eV for the EuCOT cluster and it increases to 5.70 eV for the $EuCOT_2$ cluster. Then it becomes almost a constant even as the clusters size increases further. The smooth variation of BE(n) for these multidecker sandwich clusters indicates that the bonding between the Eu atoms and COT rings are insensitive to the cluster size. Furthermore, the large binding energies of these clusters should stem from their ionic bond characteristics which provide the foundation for the formation of a large cluster.

TABLE 1. Size-Dependent Binding Energy (BE), HOMO−LUMO Gap (Gap), Calculated TMM, and Measured MM [Exp.] of Eu_nCOT_{n+1} Clusters with D_{8h} Symmetry

(n,m)	BE (eV)	gap (eV)	TMM (μ_B)	Exp.[a] (μ_B)[24]
(1,1)	3.82	1.31	7	7
(1,2)	5.70	0.64	5	13(+2 to −4)
(2,3)	5.69	0.44	12	21(+2 to −8)
(3,4)	5.69	0.27	19	28(+4 to −6)
(4,5)	5.63	0.09	26	33(+5 to −5)

[a]The values in parentheses indicate the experimental uncertainty.

Magnetic Moment of Eu_nCOT_{n+1} Clusters. The calculated local and total MMs for the clusters are shown in Figure 2. The total MM is 7 μ_B in the EuCOT cluster; however, it reduces to 5 μ_B in the $EuCOT_2$ cluster. Thereafter, the total MM increases linearly by 7 μ_B per EuCOT unit, that is, the Eu_2COT_3, Eu_3COT_4, and Eu_4COT_5 clusters have the total MMs of 12, 19, and 26 μ_B, respectively. The calculated result of the Eu_2COT_3 cluster (12 μ_B) agrees well with the recent published data by Atodiresei *et al.*[27] The linear increment of the MM of the clusters is mainly attributed to the local MM in the Eu atoms since the metal atoms predominate the MM in such multidecker sandwich clusters.[23,24] In addition, our calculations show that the Eu atoms couple ferromagnetically in the ground state. Meanwhile, the planar COT rings exhibit small opposite MMs to the Eu atoms and their values depend on the cluster size and their positions in the cluster. However, the terminal COT rings exhibit

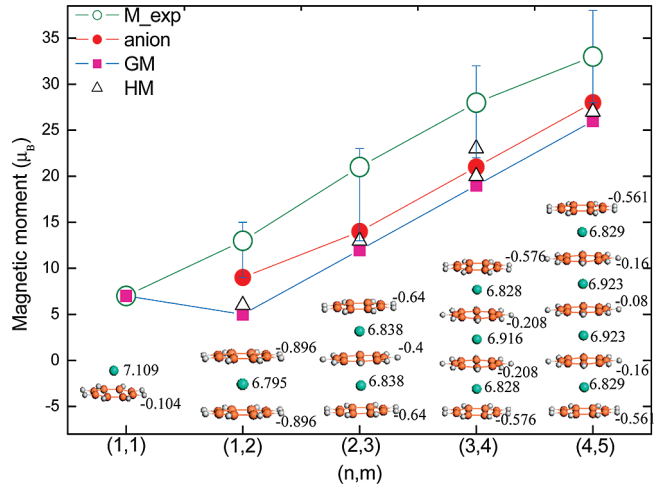

Figure 2. Calculated total MMs of the ground spin state [GM], close-energy high spin state [HM], ground anion spin state [anion], and measured MM [M_exp] of the EuCOT and Eu_nCOT_{n+1} clusters (n = 1−4) with D_{8h} symmetry. The local MMs of the Eu atoms and COT rings in the ground spin state of the neutral clusters are also presented.

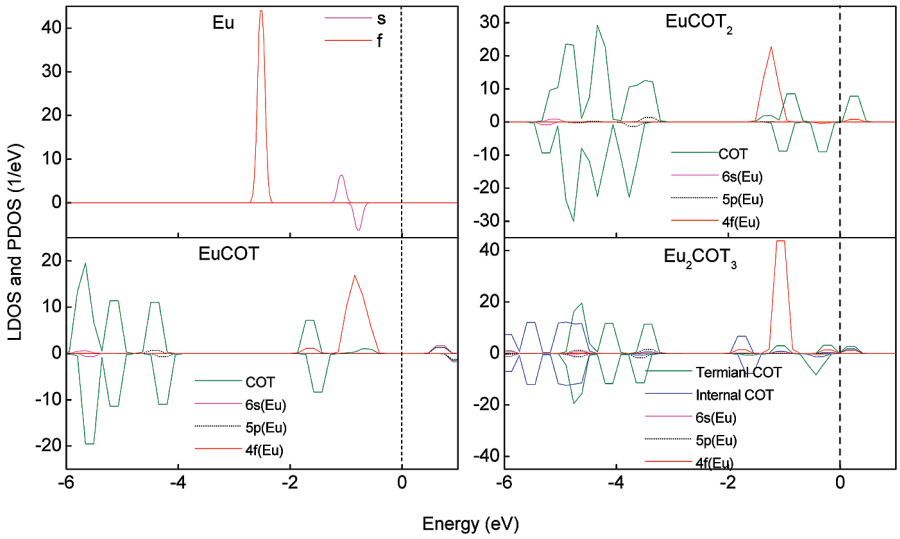

Figure 3. Local and projected density-of-states of the Eu atom, the EuCOT and Eu_nCOT_{n+1} clusters (n = 1 and 2). The vertical dash lines refer to the Fermi level which is shifted to zero.

considerably larger local MMs than those in the internal part of the cluster.

To deeply understand the mechanism behind the huge MMs of these clusters and find the rule among them, we analyze the charge transfer behavior within the clusters in detail. According to Hückel rule, the COT ring tends to capture two additional electrons from the Eu atoms to form a planar aromatic COT^{2-} ring in which appears no MM. In the EuCOT cluster, the Eu atom donates two 6s electrons to the COT ring, leaving seven 4f valence electrons aligned parallel and unpaired, which are responsible for the 7 μ_B MM of this cluster. However, in the $EuCOT_2$ cluster, each COT ring captures only one 6s electron from the Eu atom to form a COT^- ring, leaving one unpaired electron that would couple antiferromagnetically to the Eu atom. As a result, the MM of the $EuCOT_2$ cluster is reduced to 5 μ_B. Similarly for the larger clusters, the two terminal COT rings would be $-1e$ charged, which contribute an approximately -1 μ_B each (a total of -2 μ_B) to the clusters. In contrast, the $-2e$ charged internal COT rings have negligible local MMs. Thus, the total MMs of the Eu_nCOT_{n+1} clusters can be formulized as $7n - 2$ μ_B. More importantly, the charge transfer shows that the chemical bonding between the Eu atoms and COT rings are mainly ionic, similar to the $(MCp)_\infty$ wire.[14]

To gain further insight into the magnetic properties of these clusters, the local density-of-states (LDOS) of the COT rings and the s, p, and f projected density-of-states (PDOS) of the Eu atoms in the EuCOT, $EuCOT_2$, and Eu_2COT_3 clusters are plotted in Figure 3. It shows that the 4f orbitals of the Eu atoms in the clusters are rather localized in lower energy region without any spin-split. This is because the f electrons are shielded by the 5p and 6s electrons and are not easy to split in normal ligand environment. Therefore all f electrons can reside in nongenerated orbitals in parallel and exhibit extremely high MMs. This is intrinsically different from most of transition metal ligand sandwich clusters.

Meanwhile, we note that there are small nonzero spins in the internal COT rings and the nonintegral MMs of 7 μ_B on the Eu atoms (Table 2), which is due to weak covalent bonding within the clusters. As clearly seen from Figure 3, a very small overlap exists between the f orbitals of the Eu atoms and π orbitals of the COT rings, indicating weak covalent interactions inside the clusters. Moreover, the LDOS shows that the minority spins of the terminal COT rings are closer to the Fermi level and are aligned in opposite direction to the f states of the Eu atoms. It induces the negative

TABLE 2. Electronic State (ES), Total Magnetic Moment (TMM), Spin Arrangement of Different Eu Atoms (S-A), Energy Difference (ΔE) between FM and AFM States and Individual MMs of FM and AFM States for the Eu_2COT_3, Eu_3COT_4, and Eu_4COT_5 Clusters. COT1−5 and Eu1−4 Specify the COT Rings and Eu Atoms from One End to the Other End of the Cluster

					Individual MM (μ_B)								
system	ES	TMM (μ_B)	S-A	ΔE (eV)	COT1	Eu1	COT2	Eu2	COT3	Eu3	COT4	E4	COT5
(2,3)	FM	12	↑ ↑	0	−0.64	6.838	−0.4	6.838	−0.64				
	AFM_1	0	↑ ↓	0.178	−0.556	6.806	0.0	−6.806	0.556				
(3,4)	FM	19	↑ ↑ ↑	0	−0.576	6.828	−0.208	6.916	−0.208	6.828	−0.576		
	AFM_1	7	↑ ↑ ↓	0.028	−0.506	6.830	−0.168	6.912	0.032	−6.818	0.456		
	AFM_2	7	↑ ↓ ↑	0.107	−0.468	6.816	−0.064	−6.900	−0.064	6.816	−0.468		
(4,5)	FM	26	↑ ↑ ↑ ↑	0	−0.561	6.829	−0.16	6.923	−0.08	6.923	−0.16	6.829	−0.561
	AFM_1	0	↑ ↑ ↓ ↓	0.009	−0.472	6.834	−0.144	6.913	0.0	−6.913	0.144	−6.834	0.472
	AFM_2	14	↑ ↑ ↑ ↓	0.025	−0.472	6.835	−0.152	6.922	−0.064	6.919	0.04	−6.820	0.432
	AFM_3	0	↑ ↓ ↑ ↓	0.074	−0.44	6.819	−0.056	−6.906	0.0	6.906	0.056	−6.819	0.44
	AFM_4	12	↑ ↑ ↓ ↑	0.039	−0.480	6.833	−0.144	6.909	−0.019	−6.910	−0.056	6.820	−0.440
	AFM_5	0	↑ ↓ ↓ ↑	0.057	−0.440	6.820	−0.04	−6.918	0.048	−6.918	−0.04	6.820	−0.440

spins in the clusters. The DOS results are in accord with the charge transfer and local MMs analysis.

Spin Stability of Eu_nCOT_{n+1} Clusters. Besides the ferromagnetic (FM) ground state, we also identify possible antiferromagnetic (AFM) states in the Eu_nCOT_{n+1} clusters when $n \geq 2$. The local MMs of the individual Eu atoms and COT rings at their FM and AFM states for the Eu_nCOT_{n+1} clusters ($n \geq 2$) are summarized in Table 2. It is found that the energy difference (ΔE) between the FM and AFM states becomes smaller when the cluster's size increases, for example, ~0.009 eV for the Eu_4COT_5 cluster. The small energy difference implies high spin instability in these clusters. As aforementioned, the f electrons of the Eu atoms are shielded by the outer 5p and 6s electrons that keep the f orbitals nonsplit and generate huge MMs. On the other hand, the shielded f electrons in the Eu atoms result in weak coupling between the metal atoms, leading to an easy spin-flipping for the Eu atoms in the Eu_nCOT_{n+1} clusters; and eventually it may cause serious spin-instability.

In addition, it shows that the COT rings tend to couple in parallel with each other but antiparallel with the Eu atoms at the FM ground state. It implies that the double-exchange coupling between the Eu atoms is the key mechanism. For the AFM states, the coupling mechanism may be slightly complicated since they are excited state. But we believe that the double-exchange coupling mechanism still predominates in these clusters. The COT^{2-} rings act as mediators in either the ferromagnetic or antiferromagnetic couplings between the Eu^{2+} atoms.[14]

Finally, we must point out that except for the half-sandwich EuCOT cluster, the calculated MMs of these clusters are systemically lower than the experimental data (Table 1).[24] One reason for such deviation is due to the temperature effects. Our DFT calculations are done at 0 K while the experiments are carried out at 80 K. Another possibility is that under the high vacuum atmosphere and laser radiation, excitation states may accrue and various states, such as ionic or radical species, may coexist. The higher spin states plotted in Figure 2 are normally 0.19−0.36 eV higher than that of the ground state in energy. In addition, the anionic states of the clusters show even higher MMs but still lower than that observed from experiments. Meanwhile, we also note that the experimental uncertainty is extremely large. Some large values observed in experiments seem to be very unusual. For example, the reported MM of the Eu_2COT_3 cluster is 21 μ_B.[24] The systematic experimental error is also one of the possibilities to explain the deviation. Therefore, further theoretical and experimental investigations are demanded for lanthanide sandwich molecular clusters.

Bonding Characteristics in Neutral and Charged Eu_nCOT_{n+1} Clusters. As we have shown above, the interior parts of the Eu_nCOT_{n+1} clusters are of mainly ionic characteristic (Eu^{2+} and COT^{2-} ionized counterparts) due to the two electrons transferred from the Eu atoms to COT rings. However, the terminal COT rings only gain one electron and exhibit $-1e$ charge (Mulliken charge and natural population analysis (NPA) on Eu and COT are presented in Table S1 in Supporting Information, which can qualitatively reflect this characteristic), and it leads to a net antiferromagnetic coupling with the Eu atoms. Such magnetic coupling results in a very unique covalent-ionic hybrid bond between the terminal COT^{-} rings and their adjacent Eu^{2+} ions at both ends of the clusters. This can be evaluated *via* the spin density of the clusters. We take the longest cluster Eu_4COT_5 as an example (Figure 4a). For the neutral cluster, it shows that the spin density is mainly localized at the Eu atoms and almost none around the internal COT^{2-} rings due to their saturating electron number (satisfying $4n + 2$ rule). Meanwhile, the terminal COT rings exhibit significant spin density, and couple antiferromagnetically to the Eu atoms. It means the bonds between the terminal COT^{1-} rings and their adjacent Eu^{2+} ions are not purely ionic but are of hybrid covalent-ionic characteristic which show extremely strong bonding due to the antiferromagnetic coupling. This can be further verified from the bond distances. The terminal distance between the COT^{1-} ring and Eu^{2+} atom is significantly shorter than those in the interior part (Figure 4a). It can be clearly seen that the Eu_4COT_5 cluster is capped by such two hybrid covalent-ionic terminals. We believe that such unique structures in the Eu_nCOT_{n+1} clusters make them extremely stable, and subsequently to be able to form a very long 1D wire up to 18-layer. It may be the longest 1D multidecker molecular cluster synthesized up to date. In contrast, the longest transition-metal sandwich cluster is limited to ~7 layers for V_nBz_m, deriving from covalent bonding between V and Bz.[22]

Furthermore, we calculate the spin densities of the positively and negatively charged Eu_4COT_5 clusters (Figure 4a). We find that adding or removing electrons in the cluster affects the COT rings only, that is, the electron spin densities at the Eu ions do not change. When one electron is taken out from Eu_4COT_5 ($+1e$ charged), the COT rings next to the terminal rings develop some spin densities, indicating that these COT rings start to carry some antiferromagnetic spin. For the $+2e$ charged state, the spin densities are found to extend further into the internal COT rings to form deeper hybrid covalent-ionic caps. In contrast, the spin densities on the two terminal COT rings decrease when one electron is added to the cluster ($-1e$ charged). Strikingly, for the $-2e$ charged state, the spin densities on the terminal COT rings are gone, all COT rings in the cluster are now $-2e$ charged. This indicates that the whole cluster is of purely ionic structure.

We further analyze the LDOS of the charged Eu_4COT_5 cluster (Figures 4b,c). For the $-2e$ charged

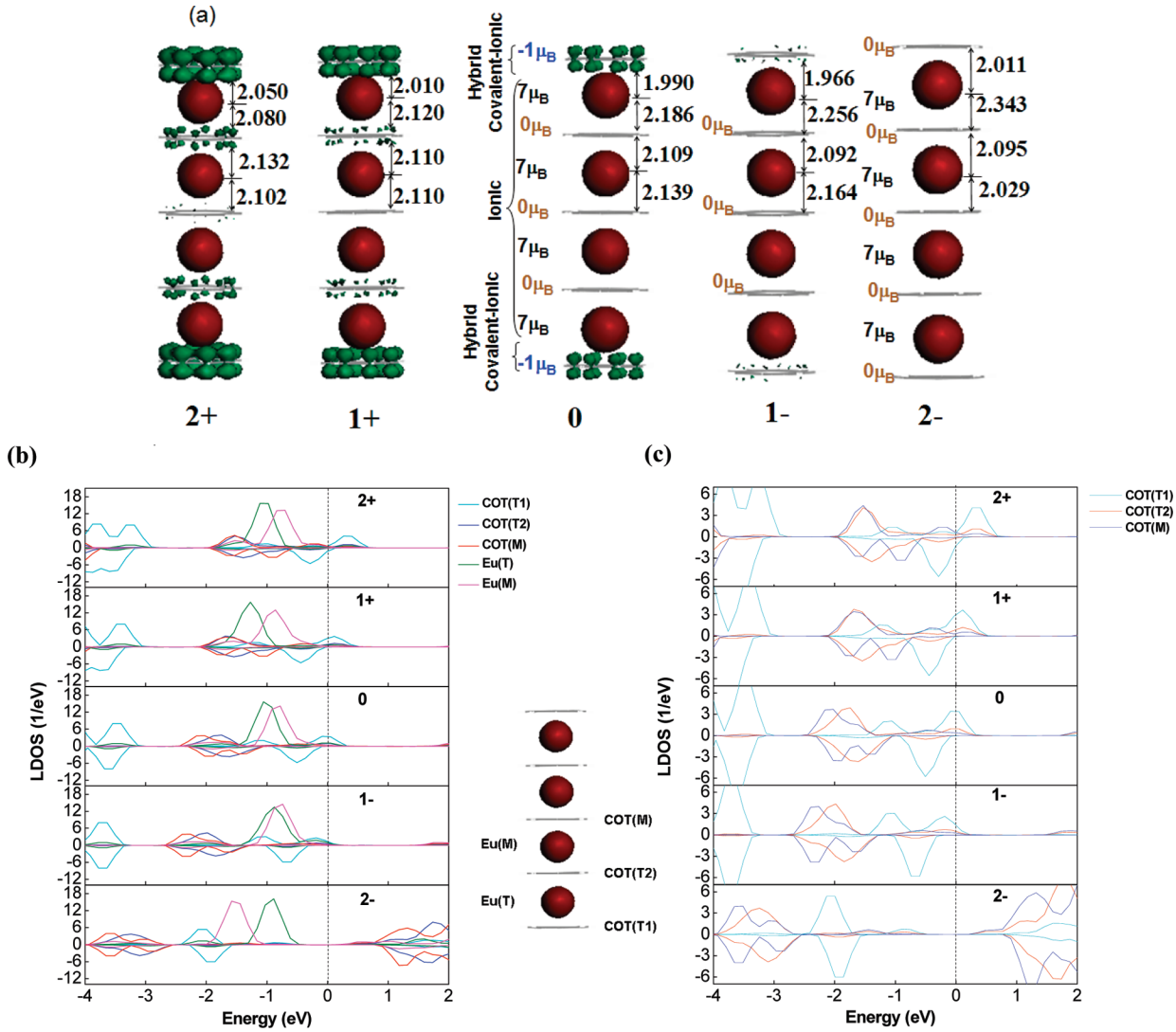

Figure 4. (a) Spin densities of the neutral and charged Eu_4COT_5 clusters. Red and green isosurfaces represent the spin densities of the Eu atoms and COT rings. (b) Local density-of-states of the neutral and charged Eu_4COT_5 clusters. The inset shows the labeling. (c) Magnified local density-of-states for the three COT rings only.

state, the major DOS of the COT rings resides at the lower energy region below that of the Eu atoms, and their majority and minority spins distribute almost symmetrically, which contributes almost zero MM to the cluster. The whole cluster is purely ionic in this case. For the $-1e$ charged state, the DOS of the terminal COT rings starts to shift toward the Fermi level. For the neutral cluster, more DOS of the terminal COT rings shifts above the Fermi level, meaning that the terminal COT rings lack electrons from the aromatic configuration. Also, the majority spin is significantly larger than the minority spin. When the cluster becomes positively charged, that is, $+1e$ and $+2e$ cases, not only the DOS of the terminal COT rings but also the DOS of the internal COT rings will shift above the Fermi level. However, the DOS of the Eu atoms still confines at around -1 eV. It indicates that the charge effect affects the COT rings only, which is consistent with the spin density analysis.

CONCLUSION

We have carried out relativistic density functional theory calculations on the half-sandwich EuCOT and full-sandwich Eu_nCOT_{n+1} ($n = 1-4$) clusters. We show that (1) these clusters are energetically stable with freely rotatable COT rings; (2) the total MMs of these clusters increase linearly with the number of Eu atoms; (3) the ferromagnetic and antiferromagnetic states of these clusters are energetically competitive, indicating that their spin states are very unstable. More importantly, we reveal (4) an interesting bonding characteristic of these clusters: an ionic-bonded interior structure capped with two hybrid covalent-ionic terminals. Such unique structures in the Eu_nCOT_{n+1} clusters make them extremely stable. In addition, we find that (5) the hybrid covalent-ionic terminals will extend toward the interior part of the cluster to form deeper covalent-ionic caps in positively charged clusters. In contrast, the negatively charged clusters show pure ionic structures. The re-

vealed properties should provide more information for designing molecular spintronics.

TABLE 3. Comparison of All-Electron DFT Results (PW91/DNP/DSPP) with Experimental (exp) and Other Theoretical (theo) Results for the Eu, COT, $EuCOT_2$, and Eu_2COT_3 Systems. IP is the Ionization Potential; R_{C-C} is the C−C Bond Length

system	properties	PW91/DNP/DSPP	earlier results
Eu	IP (eV)	5.60	5.67 (exp)[36]
COT	symmetry	S_4	S_4 (theo)[30]
	R_{C-C} (long)	1.467	1.472 (theo)[30]
	R_{C-C} (short)	1.346	1.345 (theo)[30]
	IP (eV)	8.0	8.2 ± 0.2 (exp)[37]
$EuCOT_2$	IP (eV)	6.52	5.92−6.42 (exp)[18]
Eu_2COT_3	IP (eV)	5.95	5.92−6.42 (exp)[18]

METHODS

We used the Perdew−Wang gradient-corrected functional (PW91)[31] within DFT. All-electron double numerical basis sets with polarization functions (DNP) were adopted for the C and H atoms, and the relativistic semicore pseudopotential (DSPP) was used for the Eu atom, as implemented in DMol3 package.[32] We used a three-step procedure to identify the ground state structure. First, a cluster's spin state was determined by checking the "auto" set in the DMol3 package. Next, to avoid the cluster trapped in a local-minimum spin state, various spin projection values were assigned to the cluster; geometry optimization was then reperformed for each given spin state. Finally, the lowest energy structures were further verified to be the true minima instead of the saddle points in the potential energy surface by harmonic frequency calculations. All the structures were fully optimized without symmetry constraint.

Currently, GGA+U method within Vienna *ab initio* simulation (VASP) package[33−35] is commonly used for rare-earth compounds calculations in which the localized 4f electrons play an important role. Note that VASP adopts planewave basis set approach while DMol3 uses localized orbital approach. Nevertheless, as a comparison to the method we used, we performed GGA+3.7 eV calculations using VASP for the half-sandwiched EuCOT and Eu_nCOT_{n+1} (n = 1−4) clusters based on the experimental observations[23,24] and previous theoretical work.[27] Our calculations show that the difference between two aforementioned methods for MM and structures are negligible (see Table S2 in Supporting Information). In addition, the reliability of the PW91/DNP/DSPP method is assessed by calculating the ionization potentials (IP) of the Eu atom, COT ring, and Eu_nCOT_{n+1} (n = 1 and 2) clusters. Our benchmarking results are in good agreement with experimental data as well as the previously theoretical reports (Table 3). Therefore, we expect this PW91/DNP/DSPP method is reliable for the Eu_nCOT_{n+1} calculations.

Acknowledgment. The work is supported by the National Natural Science Foundation of China (No.10604013, 20873019), NBRP of China (No. 2010CB923401, 10990100) the Program for New Century Excellent Talents in the University of China (NCET-06-0470), and the Project-sponsored by SRF for ROCS, SEM, the Qinglan Project in the University of Jiangsu Province, and the Teaching and Research Foundation for the Outstanding Young Faculty and Peiyu Foundation of Southeast University. J.W. would like to acknowledge the computational resources provided by the Department of Physics, Southeast University.

Supporting Information Available: Calculations of Mulliken charges and natural population analysis, and comparison of total energy difference between the FM and AFM states using VASP and DMol3 for the EuCOT and Eu_nCOT_{n+1} clusters. This material is available free of charge *via* the Internet at http://pubs.acs.org.

REFERENCES AND NOTES

1. Yasuike, T.; Nakajima, A.; Yabushita, S.; Kaya, K. Why Do Vanadium Atoms Form Multiple-Decker Sandwich Clusters with Benzene Molecules Efficiently? *J. Phys. Chem. A* **1997**, *101*, 5360–5367.
2. Hoshino, K.; Kurikawa, T.; Takeda, H.; Nakajima, A.; Kaya, K. Structures and Ionization Energies of Sandwich Clusters (V_n(benzene)$_m$). *J. Phys. Chem.* **1995**, *99*, 3053–3055.
3. Weis, P.; Kemper, P. R.; Bowers, M. T. Structures and Energetics of $V_n(C_6H_6)_m^+$ Clusters: Evidence for a Quintuple-Decker Sandwich. *J. Phys. Chem. A* **1997**, *101*, 8207–8213.
4. Kandalam, A. K.; Rao, B. K.; Jena, P.; Pandey, R. Geometry and Electronic Structure of $V_n(Bz)_m$ Complexes. *J. Chem. Phys.* **2004**, *120*, 10414.
5. Wang, J.; Acioli, P. H.; Jellinek, J. Structure and Magnetism of V_nBz_{n+1} Sandwich Clusters. *J. Am. Chem. Soc.* **2005**, *127*, 2812–2813.
6. Wang, J.; Jellinek, J. Infrared Spectra of V_nBz_{n+1} Sandwich Clusters: A Theoretical Study of Size Evolution. *J. Phys. Chem. A* **2005**, *109*, 10180–10182.
7. Miyajima, K.; Yabushita, S.; Knickelbein, M. B.; Nakajima, A. Stern−Gerlach Experiments of One-Dimensional Metal−Benzene Sandwich Clusters: $M_n(C_6H_6)_m$ (M = Al, Sc, Ti, and V). *J. Am. Chem. Soc.* **2007**, *129*, 8473–8480.
8. Weng, H. M.; Ozaki, T.; Terakura, K. Theoretical Analysis of Magnetic Coupling in Sandwich Clusters $V_n(C_6H_6)_{n+1}$. *J. Phys. Soc. Jpn.* **2008**, *77*, 014301.
9. Mokrousov, Y.; Atodiresei, N.; Bihlmayer, G.; Heinze, S.; Blugel, S. The Interplay of Structure and Spin-Orbit Strength in the Magnetism of Metal−Benzene Sandwiches: From Single Molecules to Infinite Wires. *Nanotechnology* **2007**, *18*, 495402.
10. Rahman, M. M.; Kasai, H.; Dy, E. S. Theoretical Investigation of Electric and Magnetic Properties of Benzene−Vanadium Sandwich Complex Chain *Jpn. J. Appl. Phys.* **2005**, *44*, 7954–7956.
11. Xiang, H. J.; Yang, J. L.; Hou, J. G.; Zhu, Q. S. One-Dimensional Transition Metal−Benzene Sandwich Polymers: Possible Ideal Conductors for Spin Transport. *J. Am. Chem. Soc.* **2006**, *128*, 2310–2314.
12. Maslyuk, V. V.; Bagrets, A.; Meded, V.; Arnold, A.; Evers, F.; Brandbyge, M.; Bredow, T.; Mertig, I. Organometallic Benzene−Vanadium Wire: A One-Dimensional Half-Metallic Ferromagnet. *Phys. Rev. Lett.* **2006**, *97*, 097201.
13. Mokrousov, Y.; Atodiresei, N.; Bihlmayer, G.; Gel, S. Magnetic Anisotropy Energies of Metal−Benzene Sandwiches. *Int. J. Quantum Chem.* **2006**, *106*, 3208–3213.
14. Shen, L.; Yang, S.-W.; Ng, M.-F.; Ligatchev, V.; Zhou, L.; Feng, Y. Charge-Transfer-Based Mechanism for Half-Metallicity and Ferromagnetism in One-Dimensional Organometallic Sandwich Molecular Wires. *J. Am. Chem. Soc.* **2008**, *130*, 13956–13960.
15. Zhou, L.; Yang, S.-W.; Ng, M.-F.; Sullivan, M. B.; Tan, V. B. C.; Shen, L. One-Dimensional Iron−Cyclopentadienyl Sandwich Molecular Wire with Half Metallic, Negative Differential Resistance and High-Spin Filter Efficiency Properties. *J. Am. Chem. Soc.* **2008**, *130*, 4023–4027.
16. Wang, L; Cai, Z.; Wang, J.; Lu, J.; Luo, G.; Lai, L.; Zhou, J.; Qin, R.; Gao, Z.; Yu, D.; Li, G.; Mei, W. N.; Sanvito, S. Novel One-Dimensional Organometallic Half Metals: Vanadium−Cyclopentadienyl, Vanadium−Cyclopentadienyl−Benzene, and Vanadium−Anthracene Wires. *Nano Lett.* **2008**, *8*, 3640–3644.

17. Zhang, X.; Wang, J.; Gao, Y.; Zeng, X. *Ab Initio* Study of Structural and Magnetic Properties of TM_n(ferrocene)$_{n+1}$ (TM = Sc, Ti, V, Mn) Sandwich Clusters and Nanowires ($n = \infty$). *ACS Nano* **2009**, *3*, 537–545.
18. Kurikawa, T.; Negishi, Y.; Satoshi, F. H.; Nagao, S.; Miyajima, K.; Nakajima, A.; Kaya, K. Multiple-Decker Sandwich Complexes of Lanthanide−1,3,5,7-Cyclooctatetraene [$Ln_n(C_8H_8)_m$] (Ln = Ce, Nd, Eu, Ho, and Yb); Localized Ionic Bonding Structure. *J. Am. Chem. Soc.* **1998**, *120*, 11766–11772.
19. Miyajima, K.; Kurikawa, T.; Hashimoto, M.; Nakajima, A.; Kaya, K. Charge Distributions in Multiple-Decker Sandwich Clusters of Lanthanide−cyclooctatetraene: Application of Na-Atom Doping. *Chem. Phys. Lett.* **1999**, *306*, 256–262.
20. Takegami, R.; Hosoya, N.; Suzumura, J.; Yada, K.; Nakajima, A.; Yabushita, S. Ionization Energies and Electron Distributions of One-End Open Sandwich Clusters: Eu_n(C8H8) $_n$ ($n = 1-4$). *Chem. Phys. Lett.* **2005**, *403*, 169–174.
21. Takegami, R.; Hosoya, N.; Suzumura, J.; Nakajima, A.; Yabushita, S. Geometric and Electronic Structures of Multiple-Decker One-End Open Sandwich Clusters: $Eu_n(C_8H_8)_n^-$ ($n = 1-4$). *J. Phys. Chem. A* **2005**, *109*, 2476–2486.
22. Hosoya, N.; Takegami, R.; Suzumura, J.; Yada, K.; Koyasu, K.; Miyajima, K.; Mitsul, M.; Knickelbein, M. B.; Yabushita, S.; Nakajima, A. Lanthanide Organometallic Sandwich Nanowires: Formation Mechanism. *J. Phys. Chem. A* **2005**, *109*, 9–12.
23. Miyajima, K.; Knickelbein, M. B.; Nakajima, A. Magnetic Properties of Lanthanide Organometallic Sandwich Complexes Produced in a Molecular Beam. *Polyhedron* **2005**, *24*, 2341–2345.
24. Miyajima, K.; Knickelbein, M. B.; Nakajima, A. Stern−Gerlach Study of Multidecker Lanthanide−Cyclooctatetraene Sandwich Clusters. *J. Phys. Chem. A* **2008**, *112*, 366–375.
25. Liu, W.; Dolg, M.; Fulde, P. Calculated Properties of Lanthanocene Anions and the Unusual Electronic Structure of Their Neutral Counterparts. *Inorg. Chem.* **1998**, *37*, 1067–1072.
26. Liu, W.; Dolg, M.; Fulde, P. Low-Lying Electronic States of Lanthanocenes and Actinocenes $M(C_8H_8)_2$ (M = Nd, Tb, Yb, U). *J. Chem. Phys.* **1997**, *107*, 3584.
27. Atodiresei, N.; Dederichs, P. H.; Mokrousov, Y.; Bergqvist, L.; Bihlmayer, G.; Blugel, S. Controlling the Magnetization Direction in Molecules *via* Their Oxidation State. *Phys. Rev. Lett.* **2006**, *100*, 117207.
28. Mallajosyula, S.; Parida, P.; Pati, S. Organometallic Vanadium−Borazine Systems: Efficient One-Dimensional Half-Metallic Spin Filters. *J. Mater. Chem.* **2009**, *19*, 1761–1766.
29. Zhu, L.; Wang, J. *Ab Initio* Study of Structural, Electronic, and Magnetic Properties of Transition Metal−Borazine Nanowires. *J. Phys. Chem. C*, in press.
30. Pierrefixe, S.; Bickelhaupt, F. Aromaticity and Antiaromaticity in 4-, 6-, 8-, and 10-Membered Conjugated Hydrocarbon Rings. *J. Phys. Chem. A* **2008**, *112*, 12816–12822.
31. Perdew, J. P.; Wang, Y. Accurate and Simple Analytic Representation of the Electron-Gas Correlation Energy. *Phys. Rev. B* **1992**, *45*, 13244.
32. DMOL is a Density Functional Theory Program Distributed by Accelrys, Inc. Delley, B. An All-Electron Numerical Method for Solving the Local Density Functional for Polyatomic Molecules. *J. Chem. Phys.* **1990**, *92*, 508. From Molecules to Solids with the $DMol^3$ Approach. J. Chem. Phys. **2000**, *113*, 7756.
33. Kresse, G.; Furthmüller, J. Efficient Iterative Schemes for *ab Initio* Total-Energy Calculations Using a Plane-Wave Basis Set. *Phys. Rev. B* **1996**, *54*, 11169.
34. Kresse, G.; Furthmüller, J. Efficiency of *ab-Initio* Total Energy Calculations for Metals and Semiconductors Using a Plane-Wave Basis Set. *Comput. Mater. Sci.* **1996**, *6*, 15–20.
35. Blochl, P. E. Projector Augmented-Wave Method. *Phys. Rev. B* **1994**, *50*, 17953.
36. NIST Standard Reference Database 69, March 2003 Release; NIST Chemistry WebBook; http://webbook.nist.gov.
37. Yang, Y.; Hsu, W.; Lee, H.; Huang, Y.; Yeh, C.; Hu, C. Experimental and Theoretical Studies of Metal Cation−Pyridine Complexes Containing Cu and Ag. *J. Phys. Chem. A* **1999**, *103*, 11287–11292.